BIOCHEMISTRY
including biophysical chemistry & molecular biology

Article

pubs.acs.org/biochemistry

Crystal Structures of Glutaminyl Cyclases (QCs) from *Drosophila melanogaster* Reveal Active Site Conservation between Insect and Mammalian QCs

Birgit Koch,[†,‡] Petr Kolenko,[§] Mirko Buchholz,[†] David Ruiz Carrillo,[†,§] Christoph Parthier,[§] Michael Wermann,[†] Jens-Ulrich Rahfeld,[†] Gunter Reuter,[∥] Stephan Schilling,*[,†] Milton T. Stubbs,*[,§] and Hans-Ulrich Demuth[†]

[†]Probiodrug AG, Weinbergweg 22, D-06120 Halle (Saale), Germany

[‡]Biosolutions GmbH, Weinbergweg 22, D-06120 Halle (Saale), Germany

[§]Institut für Biochemie und Biotechnologie, Martin-Luther-Universität Halle-Wittenberg, Kurt-Mothes-Straße 3, D-06120 Halle (Saale), Germany

[∥]Institut für Genetik, Martin-Luther-Universität Halle-Wittenberg, Weinbergweg 20, D-06120 Halle (Saale), Germany

Supporting Information

ABSTRACT: Glutaminyl cyclases (QCs), which catalyze the formation of pyroglutamic acid (pGlu) at the N-terminus of a variety of peptides and proteins, have attracted particular attention for their potential role in Alzheimer's disease. In a transgenic *Drosophila melanogaster* (*Dm*) fruit fly model, oral application of the potent competitive QC inhibitor PBD150 was shown to reduce the burden of pGlu-modified Aβ. In contrast to mammals such as humans and rodents, there are at least three *Dm*QC species, one of which (isoDromeQC) is localized to mitochondria, whereas DromeQC and an isoDromeQC splice variant possess signal peptides for secretion. Here we present the recombinant expression, characterization, and crystal structure determination of mature DromeQC and isoDromeQC, revealing an overall fold similar to that of mammalian QCs. In the case of isoDromeQC, the putative extended substrate binding site might be affected by the proximity of the N-terminal residues. PBD150 inhibition of DromeQC is roughly 1 order of magnitude weaker than that of the human and murine QCs. The inhibitor binds to isoDromeQC in a fashion similar to that observed for human QCs, whereas it adopts alternative binding modes in a DromeQC variant lacking the conserved cysteines near the active center and shows a disordered dimethoxyphenyl moiety in wild-type DromeQC, providing an explanation for the lower affinity. Our biophysical and structural data suggest that isoDromeQC and human QC are similar with regard to functional aspects. The two *Dm* enzymes represent a suitable model for further in-depth analysis of the catalytic mechanism of animal QCs, and isoDromeQC might serve as a model system for the structure-based design of potential AD therapeutics.

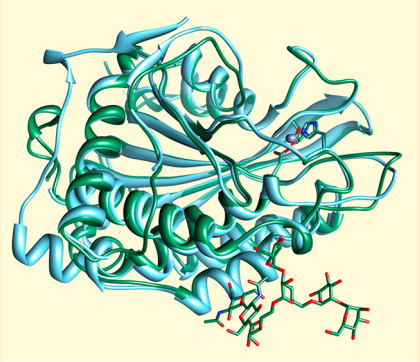

The existence of pyroglutamic acid (pGlu) at the N-termini of peptides and proteins has been described in plants and animals.[1−5] N-Terminal basicity is lost as a result of the cyclization, and peptide stability against aminopeptidase degradation is increased. Glutaminyl cyclases (QCs) catalyze the conversion of glutamine and glutamic acid into pGlu.[6,7] Whereas the enzymes of plant and bacterial origin are homologous to one another,[8−10] mammalian QCs have evolved from another ancestral precursor, most likely a bacterial zinc-dependent aminopeptidase,[11] and have been characterized as single-zinc metalloenzymes.[12,13] Mammalian QCs are highly conserved among different species, with the murine and human enzymes having >80% identical sequences, virtually identical enzymatic characteristics,[14−16] and a conserved α/β-hydrolase fold.[17] Human glutaminyl cyclase activity has been implicated in the post-translational modification of a broad range of substrates, including structural proteins such as collagen, enzymes (e.g., RNase 4), chemokines, and peptide hormones (including gonadotropin-releasing hormone[18] and thyrotropin-releasing hormone[19]). An N-terminal pGlu residue can influence the receptor active conformation of the hormones and chemokines and protect against degradation by aminopeptidases. Human glutaminyl cyclase enzymes have attracted considerable attention because of their involvement in chemokine maturation (e.g., CCL2[2]) and amyloid Aβ peptide formation [e.g., British (ABri) or Danish (ADan) amyloid] in neurodegenerative disorders.[20,21]

Initial pharmacologic studies using the compound PBD150 [1-(3,4-dimethoxyphenyl)-3-(3-imidazol-1-ylpropyl)thiourea] provided evidence of the disease-modifying potential of QC

Received: May 25, 2012
Revised: August 15, 2012
Published: August 16, 2012

dx.doi.org/10.1021/bi300687g | *Biochemistry* 2012, 51, 7383−7392

inhibition in animal and insect models with AD-like pathology.[20,21] As part of these studies, we isolated and performed an initial characterization of two glutaminyl cyclases from *Drosophila melanogaster* (*Dm*). Identified by sequence comparison, two genes annotated as CG3248 (DromeQC) and CG5976 (isoDromeQC) were obtained that encode QCs. The proteins possess secretion signals and are most likely involved in pGlu peptide formation in the secretory pathway, with the precursors of corazonin or the adipokinetic hormone as the potential substrate. An alternative transcript could be deduced from CG5976, suggesting mitochondrial localization of the corresponding isoDromeQC protein. As no mitochondrial mammalian QC has been identified until now, the potential physiological function of the mitochondrial isoDromeQC is unclear.

In our quest to characterize the role of QCs from bacteria and animals, we have undertaken the crystallization and structural determination of DromeQC and isoDromeQC. The structures with the bound inhibitor PBD150 reveal a high level of conservation in the active site with human and murine QCs, confirming *Dm*QCs as suitable model enzymes for in-depth mechanistic investigations.

MATERIALS AND METHODS

Materials. *Escherichia coli* strain DH5α was used for all cloning procedures. For expression of DromeQC, *Pichia pastoris* strain X33 (AOX1, AOX2) was used (Invitrogen, Karlsruhe, Germany), whereas *E. coli* strain M15 was used for expression of isoDromeQC (Qiagen, Hilden, Germany). Glutaminyl peptides were obtained from Bachem (Bubendorf, Switzerland) or synthesized as described previously.[13] Recombinant pyroglutamyl aminopeptidase (pGAP) was purchased from Qiagen and bovine liver glutamic acid dehydrogenase (GDH) from Sigma-Aldrich (Steinheim, Germany). Imidazole derivatives were purchased from Sigma-Aldrich, and the inhibitor PBD150 was synthesized as described previously.[22] Media required for propagation of *E. coli* as well as *P. pastoris* were prepared according to the "Fermentation Process Guidelines" and the *Pichia* manual (Invitrogen).

Isolation of Glutaminyl Cyclase Enzymes. DromeQC and isoDromeQC were cloned as described previously.[23] Briefly, the gene for DromeQC was inserted via the *Xho*I and *Not*I restriction sites into yeast expression vector pPICZαB (Invitrogen). IsoDromeQC was ligated via the *Bam*HI and *Sph*I restriction sites into *E. coli* expression vector pQE31 (Qiagen). The N-terminal His_6 tag delivered by the vector was removed by polymerase chain reaction-mediated site-directed mutagenesis according to standard polymerase chain reaction techniques (Quik-change II site-directed mutagenesis kit, Stratagene, Santa Clara, CA) using the $H6_s/H6_{as}$ primer pair (Table S1 of the Supporting Information). Cysteine → alanine replacements in both genes were achieved by the same method using the appropriate primer pairs listed in Table S1 of the Supporting Information. The cDNA sequence was verified by sequencing using vector-specific primers.

DromeQC and its corresponding mutants were expressed and purified as described previously.[23] IsoDromeQC was heterologously expressed in *E. coli* using Fernbach flasks at room temperature overnight and expression induced by addition of 0.2 mM IPTG (isopropyl β-D-1-thiogalactopyranoside). Cells were disrupted using lysozyme (1 mg/mL) and a freeze−thaw cycle. Enzymes were purified using hydrophobic interaction and anion exchange liquid chromatographic steps. QC-containing fractions were pooled, and the purity was analyzed by sodium dodecyl sulfate−polyacrylamide gel electrophoresis (Figure S1 of the Supporting Information). The purified enzyme was stored at −20 °C after addition of 50% (v/v) glycerol or without glycerol at −80 °C.

QC Assays. QC activity was assayed in 50 mM Tris-HCl (pH 8.0) essentially as described previously.[13] For spectrophotometric assessment, samples contained 30 units/mL glutamate dehydrogenase, 0.25 mM NADH/H^+ (nicotinamide adenine dinucleotide), and 15 mM α-ketoglutaric acid. Reactions were started by addition of QC, and activity was monitored by recording the decrease in absorbance at 340 nm. For fluorometric QC activity detection, reaction mixtures contained the substrate [H-Gln-βNA (β-naphthylamine) or H-Gln-AMC (7-amino-4-methylcoumarin)] and 0.4 unit/mL pyroglutamyl aminopeptidase. The excitation and emission wavelengths were 380 and 460 nm (H-Gln-AMC) or 320 and 410 nm (H-Gln-βNA), respectively. Activity was determined from a standard curve of the fluorophore under assay conditions. All determinations were conducted at 30 °C using the BMG Fluostar microplate reader (BMG Labtechnologies, Offenburg, Germany). Evaluation of all kinetic data was performed using GraFit (version 5.0.4. for windows, Erithacus software Ltd., Horley, U.K.).

For determination of the pH dependence of substrate specificity k_{cat}/K_m under first-order rate conditions, i.e., at $[S] \ll K_m$, a three-component buffer system consisting of 25 mM acetic acid, 25 mM Mes, and 50 mM Tris was applied according to the method of Ellis and Morrison,[24] providing a constant ionic strength. Rate profiles were adjusted by fitting the data according to an equation accounting for three dissociating groups (see Figure S2A of the Supporting Information).

Spectroscopic Evaluation. CD spectra were acquired using a Jasco J-715 spectropolarimeter (Jasco, Groß-Umstadt, Germany) with quartz cuvettes with a 0.1 cm path length and an external thermostat (Julabo F25, Julabo, Seelbach, Germany). Purified DromeQC and isoDromeQC were dissolved in 10 mM potassium phosphate buffer (pH 6.8). The mean of 10 scans between 190 and 260 nm was calculated and baseline corrected. To study the thermal stability, wavelength scans were performed every 10 K. The ellipticity at 223 nm was used to assess the unfolding transition. Guanidine hydrochloride (GdmCl) was used over a concentration range of 0−6 M to assess the chemical stability.

Crystallization. Crystals of both proteins and their mutants were prepared using the hanging-drop vapor diffusion method at room temperature (294 K) using 1 + 1 μL drops and 1 mL of reservoir in EasyXtal 24-well plates (Qiagen). DromeQC was concentrated to 15 mg/mL in buffer containing 100 mM NaCl, 25 mM Bis-Tris (pH 6.8), and 2 mM PBD150; the reservoir consisted of 10% (w/v) PEG 35000 and 100 mM Tris (pH 8.5) or 12% (w/v) PEG 8000 and 100 mM Mes (pH 6.5) for the mutant lacking a disulfide. IsoDromeQC was concentrated to 10 mg/mL in buffer containing 100 mM NaCl, 15 mM Bis-Tris (pH 6.8), and 2 mM PBD150; the reservoir consisted of 200 mM $MnCl_2$, 30% (w/v) PEG 4000, and 100 mM Tris (pH 8.5). The proteins crystallized within 2 weeks. Crystals were cryoprotected using 20% (v/v) glycerol, flash-frozen at a temperature of 100 K, and tested for diffraction using Cu Kα radiation (λ = 1.5418 Å) on our in-house rotating-anode source (RA Micro 007, Rigaku/MSC, Tokyo, Japan) equipped with VarimaxTM Optics and X-Stream cryo stream (Rigaku) using a CCD detector device (CCD Saturn 944+, Rigaku) mounted on an AFC-11 goniometer.

dx.doi.org/10.1021/bi300687g | *Biochemistry* 2012, 51, 7383−7392

Table 1. Summary of Crystallographic Data and Refinement Statistics[a]

	WT DromeQC	DromeQC C113A/C136A	WT isoDromeQC	isoDromeQC C136A/C158A
PDB entry	4F9U	4F9V	4FAI	4FBE
resolution (Å)	50.00−1.80 (1.90−1.80)	50.00−2.10 (2.21−2.10)	35.00−1.65 (1.74−1.65)	45.00−1.88 (1.99−1.88)
space group	$P2_1$	$P6_5$	$P1$	$P1$
unit cell parameters	a = 60.67 Å, b = 56.96 Å, c = 95.67 Å	$a = b$ = 170.87 Å, c = 57.24 Å	a = 46.44 Å, b = 47.73 Å, c = 74.56 Å	a = 45.95 Å, b = 46.44 Å, c = 74.15 Å
	$\alpha = \gamma$ = 90°, β = 108.2°	$\alpha = \gamma$ = 90°, β = 120°	α = 85.0°, β = 74.9°, γ = 73.9°	α = 84.9°, β = 75.2°, γ = 74.5°
no. of observations	237494 (33243)	210842 (30538)	275381 (39515)	71233 (3333)
completeness (%)	98.8 (97.8)	98.5 (99.1)	96.6 (95.1)	79.7 (28.5)
redundancy	4.2 (4.1)	3.8 (3.8)	4.0 (4.0)	1.9 (1.7)
R_{merge}	0.079 (0.514)	0.113 (0.678)	0.050 (0.489)	0.075 (0.342)
$I/\sigma(I)$	10.6 (2.2)	9.4 (1.9)	14.1 (2.3)	9.2 (2.4)
Wilson B factor (Å^2)	18	27	19	16
average B factor (Å^2)/no. of non-H atoms				
protein	19.3/4844	26.0/4867	21.6/4971	17.7/4947
saccharides	37.3/111	59.0/112	na[b]/0	na[b]/0
zinc ion	15.5/2	18.5/2	16.9/2	14.1/2
PBD150	33.6/44	22.8/44	26.5/44	22.2/44
solvent	29.1/579	35.0/692	30.6/448	22.3/425
total	5580	5727	5465	5418
rmsd for bond lengths from ideal (Å)	0.013	0.016	0.015	0.013
rmsd for bond angles from ideal (deg)	1.488	1.415	1.379	1.392
Ramachandran plot (no. of residues)				
favored regions	571	578	576	576
allowed regions	21	22	23	20
disallowed regions	0	0	0	0
R_{work}	0.170	0.174	0.170	0.171
R_{free}	0.225	0.215	0.202	0.223
no. of reflections for R_{free} calculation	2896 (5%)	2807 (5%)	3512 (5%)	1837 (5%)
R_{all}	0.171	0.176	0.172	0.175

[a]Values in parentheses correspond to those for the highest-resolution shell. [b]Not applicable.

Data Collection and Processing. Diffraction data were collected on beamline ID14-1 at BESSY II (Berlin, Germany) at a wavelength of 0.91841 Å, processed using XDS,[25] and scaled using SCALA[26] from the CCP4[27] program package. Four variants of the two proteins crystallized in three different crystal forms (see Table 1). All four structures contain two monomers in the asymmetric units. Initial phases for isoDromeQC were obtained by molecular replacement using PHASER[28] with human QC [36% identical sequences; Protein Data Bank (PDB) entry 2AFO, chain A[12]] as a search model. The refined structure of isoDromeQC served as a search model for DromeQC (41% identical sequences). All refinements were conducted using REFMAC5,[29] and manual rebuilding was performed using COOT.[30] Weakly defined regions of the inhibitor PBD150 in DromeQC crystals [the 3,4-dimethoxyphenyl group (see below)] were refined at an occupancy of 10%. DromeQC oligosaccharides were built manually according to the *P. pastoris* glycosylation pattern, initially using a truncated template of four oligosaccharides from the Fc fragment of mouse IgG2b (PDB entry 2RGS[31]); remaining monosaccharides were built using difference electron density as the only guideline. The stereochemistry of the structures was evaluated using MOLPROBITY,[32] and agreement with structure factors was evaluated using SFCHECK.[33] Data processing and refinement statistics are listed in Table 1; coordinates have been deposited in the RCSB PDB[34] as entries 4F9U (DromeQC), 4F9V (DromeQC C113A/C136A), 4FAI (isoDromeQC), and 4FBE (isoDromeQC C136A/C158A).

RESULTS

Kinetic and Inhibition Studies. DromeQC and isoDromeQC have sequences ∼35% identical to those of human QCs and ∼40% sequence identical to each other. Both insect enzymes and their mutants lacking cysteines could be expressed and purified according to our previously published protocol.[23] To mimic the native localization, DromeQC was heterologously expressed in the secretory pathway of *P. pastoris*, whereas isoDromeQC was isolated from *E. coli*. Both DromeQC and isoDromeQC and their variants exhibit broad substrate specificities, but with differences in the pH dependence of catalysis. DromeQC displays a very narrow pH optimum at pH 7.3. In contrast, the pH dependence of isoDromeQC activity is similar to those of murine and human QC,[23] which show broad pH optima between pH 7.5 and 8 for substrate conversion (Figure S2 and Table S2 of the Supporting Information), suggesting differences in the active site microenvironments of the two *Dm*QC species. Both enzymes convert a rather broad range of potential physiological substrates in vitro (Table 2 and Table S3 of the Supporting Information), with DromeQC showing a significantly greater potential to convert these substrates at neutral pH values. A preference of the iso-enzymes for specific substrates was not observed, suggesting that conversion of

dx.doi.org/10.1021/bi300687g | *Biochemistry* 2012, 51, 7383−7392

Table 2. Specificity Constants k_{cat}/K_m for QC-Mediated Conversion of Potential Physiological Substrates of DromeQC (A) and the Mitochondrial IsoDromeQC (B) at pH 7.0 and 8.0 and for Protein Variants Lacking Two Conserved Cysteines[a]

(A) DromeQC

	$(k_{cat}/K_m)_{WT}$ (mM^{-1} s^{-1})		$(k_{cat}/K_m)_{C113A/C136A}$ (mM^{-1} s^{-1})	
substrate	pH 8	pH 7	pH 8	pH 7
39SrpL21	27.6 ± 0.4	45.3 ± 4.0	20.2 ± 2.2	49.9 ± 4.3
rho-7	30.2 ± 1.1	53.3 ± 1.2	26.2 ± 0.7	88.0 ± 4.0
ALDH2	8.3 ± 0.4	69.0 ± 8.0	7.8 ± 0.7	73.1 ± 7.2
MCCB	22.0 ± 3.1	26.1 ± 2.6	22.8 ± 0.5	28.9 ± 2.8
Acp33A	36.9 ± 0.3		35.0 ± 3.2	
DIM-10	31.2 ± 2.4	43.3 ± 3.7	59.3 ± 5.1	50.7 ± 2.8
NPLP4	20.9 ± 2.2	7.4 ± 1.0	23.8 ± 4.3	6.0 ± 0.4

(B) IsoDromeQC

	$(k_{cat}/K_m)_{WT}$ (mM^{-1} s^{-1})		$(k_{cat}/K_m)_{C136A/C158A}$ (mM^{-1} s^{-1})	
substrate	pH 8	pH 7	pH 8	pH 7
39SrpL21	21.1 ± 0.3	21.9 ± 0.7	15.9 ± 1.1	20.9 ± 0.5
rho-7	43.4 ± 4.1	55.0 ± 2.6	40.9 ± 1.1	50.2 ± 4.6
ALDH2	33.9 ± 1.9	32.0 ± 3.3	26.2 ± 2.8	40.9 ± 7.4
MCCB	33.2 ± 0.7	25.5 ± 3.7	32.3 ± 1.1	25.0 ± 1.7
Acp33A	36.0 ± 7.0		38.0 ± 6.0	
DIM-10	17.5 ± 2.0	25.9 ± 2.5	13.9 ± 1.5	31.2 ± 4.0
NPLP4	21.5 ± 1.4	4.2 ± 0.4	20.1 ± 1.0	4.6 ± 0.4

[a]Kinetic parameters (mean ± SD) were calculated from three independent determinations. Reactions were conducted at 30 °C in 50 mM Tris (pH 8) or 50 mM Mops (pH 7). Colocalized substrates are shown in bold. For a description of each substrate, refer to Table S3 of the Supporting Information.

different substrates is a result of in vivo colocalization, similar to that of the human iso-enzymes.[2] None of the QCs characterized so far show a restricted substrate conversion in vitro, indicating a common active site environment.

Role of Disulfide Bonds. Previous studies of murine and human QC suggested an influence of formation of the disulfide between two conserved cysteine residues on stability and/or activity.[17,35] To assess potential reasons for the differences in activity and pH dependence of *Dm*QCs, we generated mutants of both cysteine residues, DromeQC C113A/C136A and isoDromeQC C163A/C158A, which could be expressed and isolated as the WT enzymes. No large differences in kinetic behavior could be detected between the WT enzymes and their mutants (Figure 1A and Table S4 of the Supporting Information). Some lowering of the k_{cat}/K_m value was observed with DromeQC at pH 8 for the dipeptide surrogate Q-AMC and QG, and we observed 2−3-fold increased K_i values with the DromeQC mutant at pH 8. Likewise, lower specificity constants were determined for conversion of some peptide substrates (Table 2). No difference in K_i values for either DromeQC variant could be observed at pH 7 (Figure 2A and Table S5 of the Supporting Information). This slight effect on activity and inhibitor binding upon mutation of cysteine into alanine contrasts with that seen in human QC.[17] For isoDromeQC, exchange of the cysteines did not produce an influence on catalysis or inhibitor binding (Figures 1B and 2B and Tables S4 and S5 of the Supporting Information).

In human QCs, the disulfide bond is responsible for structural stabilization but does not influence activity.[17] The conformational stabilities of DromeQC and isoDromeQC and their variants were explored using CD spectroscopic analysis. The far-UV CD spectra of the two WT enzymes are virtually identical (Figure 3A). Thermally induced unfolding of DromeQC WT and variant C113A/C136A showed a significant difference in the degree of structural changes (Figure 3B), although the transition temperature of ∼50 °C did not differ. This is in contrast to deletion of the disulfide bond in hQC, which results in a reduction of the inflection temperature but similar magnitudes of signal loss for hQC WT and the corresponding Cys → Ala variants.[17] Thermal unfolding of isoDromeQC (Figure 3C) was identical for the WT and the mutant enzyme, with an inflection of the unfolding curves between 51 and 52 °C, suggesting that a Cys → Ala mutation has no influence on the stability of the enzyme.

Chemical denaturation was also monitored using guanidine hydrochloride (GdmCl)-induced unfolding via CD spectroscopy (Figure 4). Removal of the cysteines led to a reduction in conformational stability for DromeQC, with inflection points at 2.49 ± 0.03 M (WT) and 2.17 ± 0.03 M (C113A/C136A) GdmCl. A similar effect was observed with the respective hQC variants, where the inflection GdmCl concentration shifted also by 0.3 M from 3.2 M (WT) to 2.9 M (Cys → Ala) (Figure 4C). No such differences were observed for the isoDromeQC variants, each of which shows an inflection of the unfolding curves at a GdmCl concentration of 3 M (Figure 4B).

Surprisingly, significant structural changes were observed for DromeQC upon metal ion depletion (Figure S3A of the Supporting Information), in contrast to little or no differences for isoDromeQC and hQC (Figure S3B,C of the Supporting

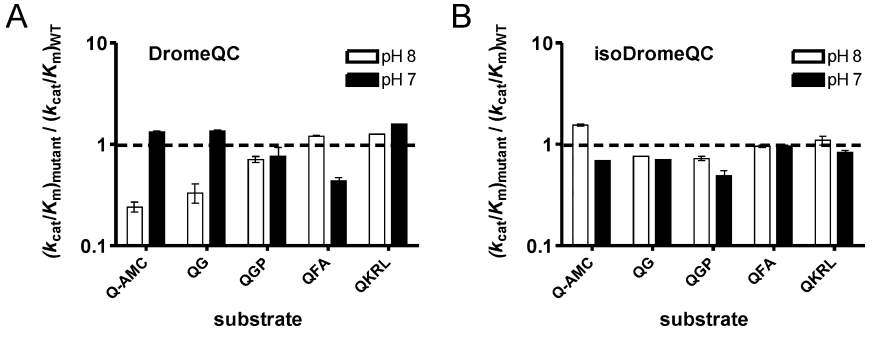

Figure 1. Relative specificity constants of WT DromeQC and its variant lacking a disulfide bond (C113A/C136A) (A) or of isoDromeQC and its C136A/C158A variant (B) at pH 8 (white bars) or pH 7 (black bars). Ratios ± SD were calculated on the basis of K_m and k_{cat} values, determined by three independent approaches. Reactions were conducted in 50 mM Tris (pH 8.0) at 30 °C.

dx.doi.org/10.1021/bi300687g | *Biochemistry* 2012, 51, 7383−7392

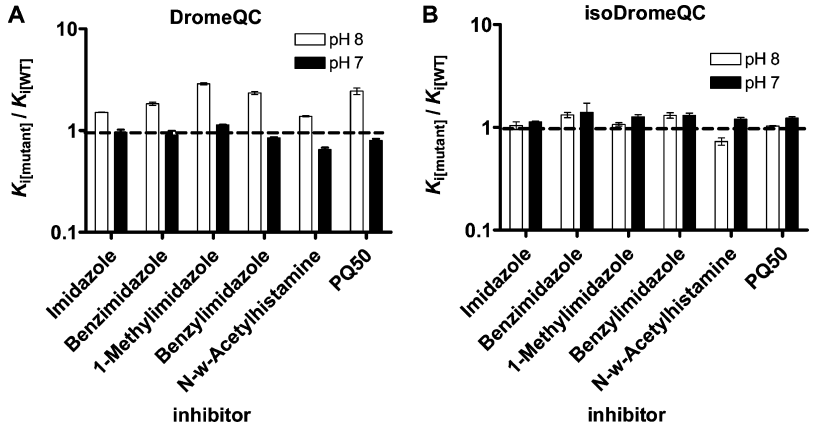

Figure 2. Ratio of inhibition constants K_i obtained with several competitive inhibitors of DromeQC and its C113A/C136A variant (A) or isoDromeQC and its C136A/C158A variant (B) at pH 8 (white bars) or pH 7 (black bars). Ratios ± SD were calculated from three independent approaches. Reactions were conducted in 50 mM Tris (pH 8.0) or 50 mM Mops (pH 7) at 30 °C.

Information), indicating differential roles of the zinc ion for structural stabilization among these enzymes.

Overall Structures of DromeQC and IsoDromeQC. Each crystal form contains two independent monomers in the asymmetric unit. The enzymes share the common globular α/β-hydrolase fold[36] (Figure 5), whose central motif consists of a twisted central β-sheet, composed of five parallel β-strands (β_1 and β_3–β_6) and one antiparallel β-strand (β_2). The β-sheets are flanked by α-helices, two helices (α_5 and α_7) filling the concave face, seven helices (α_1–α_5, α_8, and α_9) shielding the convex face of the blade, and α_6 at one edge. Similar to QC, isohQC, and mQC, isoDromeQC possesses two N-terminal α-helices (α_0 and α_1) that seal the vertex of the central β-sheet; α_0 is not present in DromeQC because of a shorter N-terminal sequence (Figure 5 and Figure S4 of the Supporting Information). The mammalian QCs also possess an additional N-terminal helix (α_{-1}) that lies over the back surface of the enzyme; this region is uncovered in isoDromeQC, whereas it is occupied in DromeQC by the extended C-terminus (albeit in two alternative conformations). Whereas the significance of this observation is not clear, loop residues of this underlying back surface appear to adopt multiple conformations in all animal QCs. Finally, isoDromeQC possesses two additional antiparallel β-strands (β_0 and $\beta_{5/6}$) at the edge of the central β-sheet joining the N-terminus of the polypeptide chain with the loop region between α-helices α_6 and α_7.

Each enzyme accommodates a catalytic zinc ion coordinated by three amino acid residues corresponding to DromeQC D131 OD2 (D153 in isoDromeQC, D159 in hQC), E171 OE2 (E191 in isoDromeQC, E202 in hQC), and H297 NE2 (H318 in isoDromeQC, H330 in hQC). In a noteworthy analogy to the known mammalian QC crystal structures, a non-proline *cis* peptide bond corresponding to the hQC D159–S160 bond is conserved in both proteins between residues D131 and S132 (DromeQC) and residues D153 and S154 (isoDromeQC), stabilized via a hydrogen bonding network.

Oligosaccharides in DromeQC. DromeQC possesses two potential N-glycosylation sites at N42 and N156. Expression in the secretory yeast *P. pastoris* resulted in glycosylation at a single site close to the N-terminus, N42 (Figure 5A). MALDI-TOF mass spectrometric analyses (not shown) confirm that N156 is not modified. Density for up to seven carbohydrate moieties could be identified, with the deduced sequence [Manα(1→2)Manα(1→6)][Manα(1→3)]Manα(1→6)Manβ(1→4)-βGlcNAc(1→4)βGlcNAc-N42 for WT DromeQC as well as [Manα(1→3)Manα(1→6)][Manα(1→2)Manα(1→3)]-Manβ(1→4)βGlcNAc(1→4)βGlcNAc-N42 for the Cys → Ala variant, typical for high-mannose glycosylation in yeast[37] and insects[38] (Figure S5 of the Supporting Information). The oligosaccharide chain is >10 Å from the active site, consistent with the lack of any decrease in activity upon deglycosylation (not shown), as also observed for hQC.[17] The glycosyl chain adopts different conformations depending on its position in the crystal, suggesting that it could cover or sequester solvent from extensive neighboring hydrophobic surface patches, providing an explanation for the significant decrease in solubility observed upon deglycosylation of DromeQC (data not shown).

Inhibition by PBD150. Both proteins and their variants were cocrystallized with the inhibitor PBD150, whose in vitro inhibitory constants are listed in Table 3. For isoDromeQC, clear electron density is visible for all atoms of inhibitor PBD150 in both chains (Figure 6D). PBD150 N3 of the imidazole moiety binds to the active site Zn^{2+}, and the propyl group fills the cavity of the active site. The orientation of the 3,4-dimethoxyphenyl part is stabilized by π–π interactions with F313 close to the active site. A water molecule that interacts with both methoxy groups was clearly identified in electron density maps. The absence of any crystal contacts in the neighborhood of the inhibitor supports this binding mode as the dominant interaction with isoDromeQC.

Despite considerable structural similarity and sequence identity near the active site, in WT DromeQC crystals, PBD150 displays significantly higher flexibility of the 3,4-dimethoxyphenyl group, for which no (chain A) or only very weak (chain B) electron density is observed (Figure 6A). Surprisingly, the inhibitor is almost completely defined in the hexagonal ($P6_5$) crystals of the DromeQC Cys → Ala variant (Figure 6B,C), which appears to be influenced by crystal packing: the dimethoxyphenyl moiety appears to be pinned by a stacking interaction to the F89 side chain of a symmetry-related molecule (Figure S6 of the Supporting Information). In this case, the 3,4-dimethoxyphenyl group adopts the same water-mediated binding mode observed with isoDromeQC, shared also by hQC and isohQC[39] but different from that of mQC.[17] The thiourea group, however, adopts two clear alternative positions, one corresponding to that observed in the human isoenzymes and the other to that in mQC (Figure 7). Similar to what has been described previously for mQC,[17] minor structural

dx.doi.org/10.1021/bi300687g | *Biochemistry* 2012, 51, 7383–7392

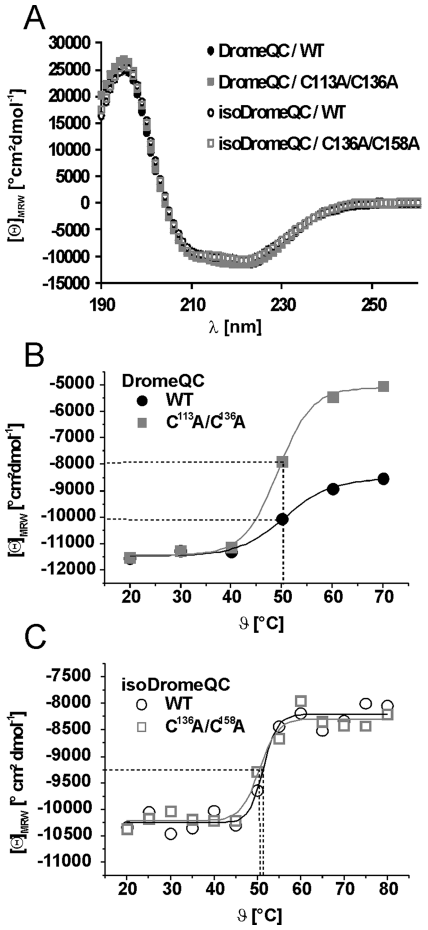

Figure 3. (A) Superposition of the far-UV CD spectra of DromeQC and isoDromeQC and their cysteine lacking variants at 20 °C, indicating highly similar structures. (B) Thermal stability assessed by a temperature-dependent change in the mean residue ellipticity at 223 nm of DromeQC WT (filled black circles) and DromeQC variant C113A/C136A lacking a disulfide bond (filled gray squares). The disulfide bridge prevents the complete structural loss of DromeQC. (C) Thermal stability observed by a temperature-dependent change in the mean residue ellipticity at 227 nm of WT isoDromeQC (empty black circles) and its C136A/C158A variant (empty gray squares). No influence on thermal stability was detected upon replacement of the cysteine residues. Proteins were dissolved in 10 mM potassium phosphate buffer (pH 6.8).

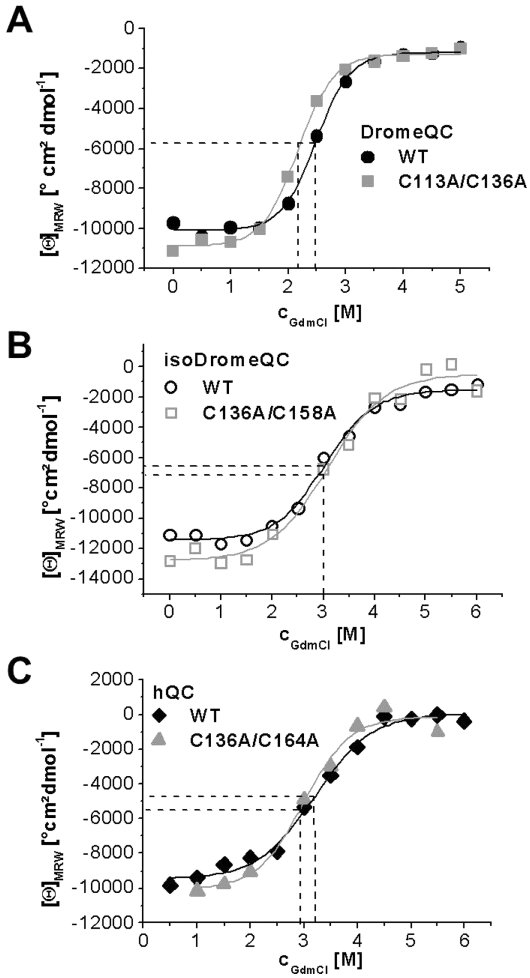

Figure 4. Conformational stability of DromeQC (A), isoDromeQC (B), and hQC (C) toward GdmCl-induced unfolding. For the natively disulfide-bridged QCs (DromeQC, hQC), conformational stability is reduced by elimination of the linkage between β-strand β_3 and α-helix α_3. This is not observed for isoDromeQC, which is natively not disulfide-linked.

rearrangements of the loop of residues 261−267 take place upon extended inhibitor binding.

DISCUSSION

N-Terminal pyroglutamic acid (pGlu) is generated during maturation of several secreted peptides and proteins, catalyzed by QCs that accept glutaminyl and, to a lesser extent, glutamyl precursors as substrates.[40] Formation of pGlu at the N-terminus stabilizes peptides against N-terminal degradation and has been shown to accelerate aggregation of amyloid peptides such as amyloid-β (Aβ) or Danish (ADan) and British (ABri) amyloid,[41,42] making QCs a focus for drug development for the reduction of pGlu-amyloid formation as a therapeutic strategy for neurodegenerative disorders.[20,21,43] This is the first structure−function analysis of invertebrate QCs and their inhibition, important for evaluating the transgenic *D. melanogaster* disease development model shown previously to be effectively treated using the inhibitor PBD150.[20]

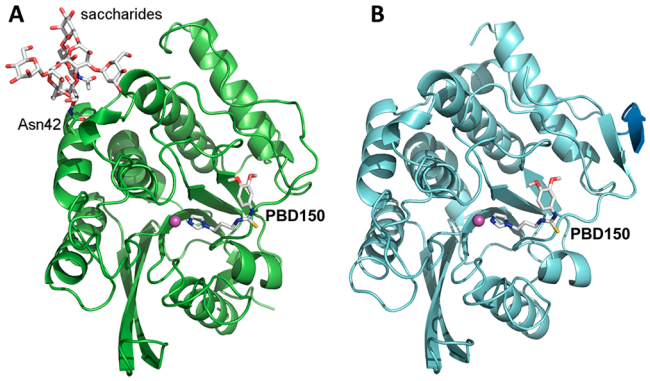

Figure 5. Structures of *Dm*QCs in complex with PBD150. (A) Overall structure of glycosylated DromeQC. (B) Overall structure of isoDromeQC. The N-terminal region of isoDromeQC (sky blue) exhibits significant structural differences. The purple spheres represent the catalytic zinc ions; inhibitor PBD150 and DromeQC oligosaccharides are represented as sticks.

The active sites of the animal QCs compared here (hQC,[12] isohQC,[39] mQC,[17] DromeQC, and isoDromeQC) show a high

dx.doi.org/10.1021/bi300687g | *Biochemistry* 2012, 51, 7383−7392

Table 3. Inhibition Constants K_i of PBD150, Determined with DromeQC, IsoDromeQC, hQC, and mQC at Different pH Values[a]

	DromeQC	isoDromeQC	hQC	mQC
pH 8	3139 ± 51	109.3 ± 9.4	102.8 ± 9.3	156.9 ± 16.8
pH 7	944 ± 93	101.3 ± 0.2	70.6 ± 3.2	222.1 ± 6.3
pH 6	2480 ± 25	370.6 ± 5.2	400.8 ± 26.8	646.3 ± 28.1

[a] K_i values (in nanomolar) are represented as means ± SD from three independent determinations. Reactions were conducted at 30°C in 50 mM Tris (pH 8), 50 mM Mops (pH 7), or 50 mM Mes (pH 6).

degree of conservation. All structures with the inhibitor PBD150 reveal a common mode of binding of the imidazole-propyl part of the inhibitor, dominated by the primary active site zinc ion interaction. IsoDromeQC exhibits an affinity for PBD150 similar to those of hQC, isohQC, and mQC (see Table 3), with a binding mode almost identical to that observed in hQC and isohQC (Figure 7). As observed for the mammalian QCs,[17,39] the imidazole ring coordinates the active site Zn^{2+} ion, with the thiourea group juxtaposing the backbone amide of E292. As in the human glutaminyl cyclases,[39] the aromatic part of the inhibitor is stabilized through interactions with isoDromeQC F313 (F325 in hQC and F346 in isohQC) and a water molecule mediated contact to both methoxy groups. Although the imidazole ring and propyl part of PBD150 adopt the same conformation in the active site of DromeQC, the lack of electron density for the 3,4-dimethoxyphenyl group in crystals of WT DromeQC is consistent with the significantly weaker binding of PBD150 (Figure 6A). Interestingly, an isohQC/hQC-like binding mode is observed in crystals of the Cys → Ala DromeQC variant, although we attribute this to crystal packing effects rather than the loss of the disulfide bridge, a conclusion supported by the K_i values determined in solution (compare

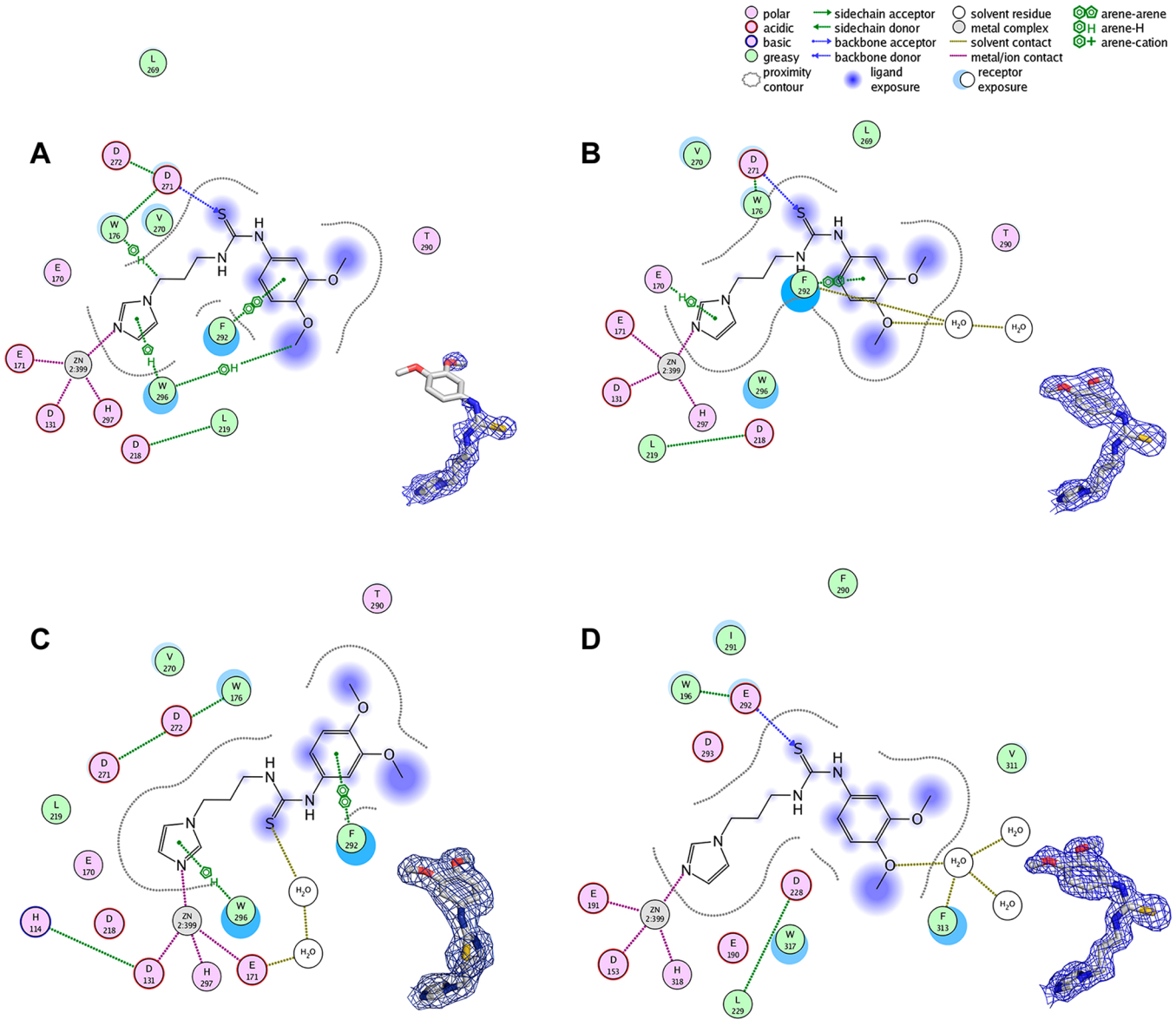

Figure 6. Binding modes of the potent inhibitor PBD150 observed in crystal structures of *Dm*QCs. (A) WT DromeQC, (B and C) DromeQC C113A/C136A variant, chains A and B, and (D) isoDromeQC. In each case, the interaction modes contributing to the ligand binding are displayed schematically, together with the $2F_o - F_c$ electron density of the inhibitor (insets) at a contour level of 1σ. The corresponding average *B* factors are listed in Table 1.

dx.doi.org/10.1021/bi300687g | *Biochemistry* 2012, 51, 7383−7392

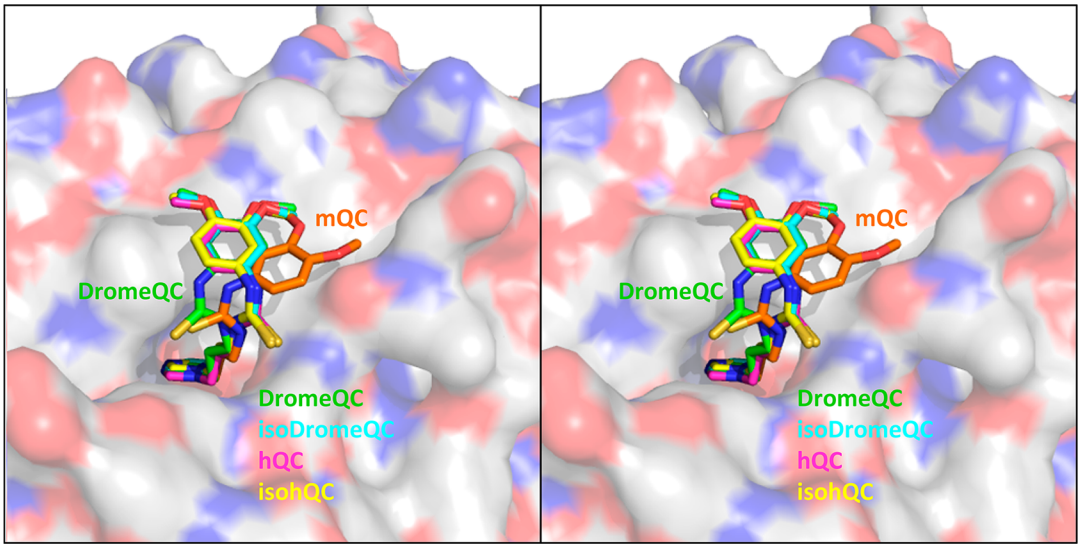

Figure 7. Overlay of the binding modes of the potent inhibitor PBD150 observed with mammalian and insect QCs in stereo. Because of a very high degree of structural similarity of the proteins, only the DromeQC surface is displayed. Inhibitor PBD150 is colored according to the protein structure (DromeQC C113A/C136A colored green, isoDromeQC colored cyan, hQC colored magenta, isohQC colored yellow, and mQC colored orange). In spite of the significant homology among the compared proteins, PBD150 can interact differently with the large hydrophobic groove adjacent to the active site.

Figure 2, Table 3, and Table S5 of the Supporting Information). The minor differences in catalytic activity and inhibitory binding between WT DromeQC and its Cys → Ala variant suggest small changes in the active site architecture that we are unable to detect in crystal structures. This is in contrast to the secreted enzymes hQC[17] and isoDromeQC studied so far, which are stabilized by the disulfide bridge, and may be correlated with the observed dependency of DromeQC stability on metal ion binding.

Apparently, the interaction with the thiourea moiety of PBD150 does not contribute to affinity significantly, as this adopts two different orientations (Figure 6B,C). Strikingly, the alternative orientation of PBD150 was also observed with mQC,[17] where the aromatic group exerts a CH−π interaction with the side chain of I304. Although the 3,4-dimethoxyphenyl group clearly contributes to the affinity of PBD150 for animal QCs, the extent is difficult to quantify as a result of the observed structural plasticity of the binding site.

Although isoDromeQC shows a generally lower specificity constant than hQC, catalysis exhibits a very similar pH dependency (Figure S2 of the Supporting Information). While we are currently unable to explain the difference in the catalytic activity, cocrystallization with the QC inhibitor PBD150, developed for hQC and possessing similar efficacy against isoDromeQC, provides further evidence of the similarity of isoDromeQC and human QCs. Notably, the inhibitory potency of PBD150 appears to depend critically on the binding mode of the 3,4-dimethoxyphenyl part of the inhibitor, which makes hydrogen bond interactions with hQC, isohQC, and isoDromeQC but shows high flexibility in DromeQC. We conclude that isoDromeQC is closely related to the human QC enzymes with respect to structural and enzymatic properties. The ease of recombinant expression and isolation of the isoDromeQC enzyme makes the enzyme well suited for in-depth analyses of catalytic function by, e.g., isotope effects, metal ion substitutions, and spectroscopic analyses. Such studies, in combination with additional structural investigations, will yield a deeper understanding of the reaction mechanism of QC enzymes and in conjunction with biological testing in transgenic fly models[20] might assist in the development of novel approaches to the treatment of Alzheimer's disease in humans.

■ ASSOCIATED CONTENT

Ⓢ Supporting Information

Experimental details concerning the expression, substrate specificity, pH dependency, and overall stability of the enzymes and more detailed information about the X-ray structures. This material is available free of charge via the Internet at http://pubs.acs.org.

■ AUTHOR INFORMATION

Corresponding Author

*S.S.: Probiodrug AG, Weinbergweg 22, D-06120 Halle (S), Germany; telephone, +49 345 5559900; fax, +49 345 5559901; e-mail, stephan.schilling@probiodrug.de. M.T.S.: Institut für Biochemie and Biotechnologie, Martin-Luther-Universität Halle-Wittenberg, Kurt-Mothes-Straße 3, D-06120 Halle (S), Germany; telephone, +49 345 55 24901; fax, +49 345 55 27360; e-mail, stubbs@biochemtech.uni-halle.de.

Author Contributions

B.K. and P.K. contributed equally to this work.

Notes

The following authors declare a potential conflict of interest: B.K., M.B., D.R.C., M.W., J.-U.R., and S.S. have been employees of Probiodrug while preparing the data for this paper. H.-U.D. serves as CSO of Probiodrug and holds stocks of the Probiodrug group.

■ ABBREVIATIONS

hQC, secreted human glutaminyl cyclase; isohQC, Golgi-resident human glutaminyl cyclase; *Dm*QC, glutaminyl cyclase of *D. melanogaster*; DromeQC, secreted glutaminyl cyclase of *D. melanogaster*; isoDromeQC, mitochondrial glutaminyl cyclase of *D. melanogaster*; mQC, secreted murine glutaminyl cyclase; PBD150, 1-(3,4-dimethoxyphenyl)-3-(3-imidazol-1-ylpropyl)-thiourea; SD, standard deviation.

REFERENCES

(1) Abraham, G. N., and Podell, D. N. (1981) Pyroglutamic acid. Nonmetabolic formation, function in proteins and peptides, and characteristics of the enzymes effecting its removal. *Mol. Cell. Biochem. 38* (Spec. No.), 181−190.

(2) Cynis, H., Hoffmann, T., Friedrich, D., Kehlen, A., Gans, K., Kleinschmidt, M., Rahfeld, J. U., Wolf, R., Wermann, M., Stephan, A., Haegele, M., Sedlmeier, R., Graubner, S., Jagla, W., Muller, A., Eichentopf, R., Heiser, U., Seifert, F., Quax, P. H., de Vries, M. R., Hesse, I., Trautwein, D., Wollert, U., Berg, S., Freyse, E. J., Schilling, S., and Demuth, H. U. (2011) The isoenzyme of glutaminyl cyclase is an important regulator of monocyte infiltration under inflammatory conditions. *EMBO Mol. Med. 3*, 545−558.

(3) Joosten, M. H., Bergmans, C. J., Meulenhoff, E. J., Cornelissen, B. J., and De Wit, P. J. (1990) Purification and Serological Characterization of Three Basic 15-Kilodalton Pathogenesis-Related Proteins from Tomato. *Plant Physiol. 94*, 585−591.

(4) Morty, R. E., Bulau, P., Pelle, R., Wilk, S., and Abe, K. (2006) Pyroglutamyl peptidase type I from *Trypanosoma brucei*: A new virulence factor from African trypanosomes that de-blocks regulatory peptides in the plasma of infected hosts. *Biochem. J. 394*, 635−645.

(5) Rep, M., Dekker, H. L., Vossen, J. H., de Boer, A. D., Houterman, P. M., Speijer, D., Back, J. W., de Koster, C. G., and Cornelissen, B. J. (2002) Mass spectrometric identification of isoforms of PR proteins in xylem sap of fungus-infected tomato. *Plant Physiol. 130*, 904−917.

(6) Fischer, W. H., and Spiess, J. (1987) Identification of a mammalian glutaminyl cyclase converting glutaminyl into pyroglutamyl peptides. *Proc. Natl. Acad. Sci. U.S.A. 84*, 3628−3632.

(7) Messer, M., and Ottesen, M. (1964) Isolation and properties of glutamine cyclotransferase of dried papaya latex. *Biochim. Biophys. Acta 92*, 409−411.

(8) Carrillo, D. R., Parthier, C., Janckel, N., Grandke, J., Stelter, M., Schilling, S., Boehme, M., Neumann, P., Wolf, R., Demuth, H. U., Stubbs, M. T., and Rahfeld, J. U. (2010) Kinetic and structural characterization of bacterial glutaminyl cyclases from *Zymomonas mobilis* and *Myxococcus xanthus*. *Biol. Chem. 391*, 1419−1428.

(9) Guevara, T., Mallorqui-Fernandez, N., Garcia-Castellanos, R., Garcia-Pique, S., Ebert, P. G., Lauritzen, C., Pedersen, J., Arnau, J., Gomis-Ruth, F. X., and Sola, M. (2006) Papaya glutamine cyclotransferase shows a singular five-fold β-propeller architecture that suggests a novel reaction mechanism. *Biol. Chem. 387*, 1479−1486.

(10) Wintjens, R., Belrhali, H., Clantin, B., Azarkan, M., Bompard, C., Baeyens-Volant, D., Looze, Y., and Villeret, V. (2006) Crystal structure of papaya glutaminyl cyclase, an archetype for plant and bacterial glutaminyl cyclases. *J. Mol. Biol. 357*, 457−470.

(11) Booth, R. E., Lovell, S. C., Misquitta, S. A., and Bateman, R. C., Jr. (2004) Human glutaminyl cyclase and bacterial zinc aminopeptidase share a common fold and active site. *BMC Biol. 2*, 2.

(12) Huang, K. F., Liu, Y. L., Cheng, W. J., Ko, T. P., and Wang, A. H. (2005) Crystal structures of human glutaminyl cyclase, an enzyme responsible for protein N-terminal pyroglutamate formation. *Proc. Natl. Acad. Sci. U.S.A. 102*, 13117−13122.

(13) Schilling, S., Niestroj, A. J., Rahfeld, J.-U., Hoffmann, T., Wermann, M., Zunkel, K., Wasternack, C., and Demuth, H.-U. (2003) Identification of Human Glutaminyl Cyclase as a Metalloenzyme: Inhibition by Imidazole Derivatives and Heterocyclic Chelators. *J. Biol. Chem. 278*, 49773−49779.

(14) Schilling, S., Cynis, H., von Bohlen, A., Hoffmann, T., Wermann, M., Heiser, U., Buchholz, M., Zunkel, K., and Demuth, H. U. (2005) Isolation, catalytic properties, and competitive inhibitors of the zinc-dependent murine glutaminyl cyclase. *Biochemistry 44*, 13415−13424.

(15) Cynis, H., Rahfeld, J. U., Stephan, A., Kehlen, A., Koch, B., Wermann, M., Demuth, H. U., and Schilling, S. (2008) Isolation of an isoenzyme of human glutaminyl cyclase: Retention in the Golgi complex suggests involvement in the protein maturation machinery. *J. Mol. Biol. 379*, 966−980.

(16) Stephan, A., Wermann, M., von Bohlen, A., Koch, B., Cynis, H., Demuth, H. U., and Schilling, S. (2009) Mammalian glutaminyl cyclases and their isoenzymes have identical enzymatic characteristics. *FEBS J. 276*, 6522−6536.

(17) Ruiz Carrillo, D., Koch, B., Parthier, C., Wermann, M., Dambe, T., Buchholz, M., Ludwig, H. H., Heiser, U., Rahfeld, J. U., Stubbs, M. T., Schilling, S., and Demuth, H. U. (2011) Structures of Glycosylated Mammalian Glutaminyl Cyclases Reveal Conformational Variability near the Active Center. *Biochemistry 50*, 6280−6288.

(18) Tan, L., and Rousseau, P. (1982) The chemical identity of the immunoreactive LHRH-like peptide biosynthesized in the human placenta. *Biochem. Biophys. Res. Commun. 109*, 1061−1071.

(19) Goren, H. J., Bauce, L. G., and Vale, W. (1977) Forces and structural limitations of binding of thyrotrophin-releasing factor to the thyrotrophin-releasing receptor: The pyroglutamic acid moiety. *Mol. Pharmacol. 13*, 606−614.

(20) Schilling, S., Zeitschel, U., Hoffmann, T., Heiser, U., Francke, M., Kehlen, A., Holzer, M., Hutter-Paier, B., Prokesch, M., Windisch, M., Jagla, W., Schlenzig, D., Lindner, C., Rudolph, T., Reuter, G., Cynis, H., Montag, D., Demuth, H. U., and Rossner, S. (2008) Glutaminyl cyclase inhibition attenuates pyroglutamate Aβ and Alzheimer's disease-like pathology. *Nat. Med. 14*, 1106−1111.

(21) Schilling, S., Appl, T., Hoffmann, T., Cynis, H., Schulz, K., Jagla, W., Friedrich, D., Wermann, M., Buchholz, M., Heiser, U., von Horsten, S., and Demuth, H. U. (2008) Inhibition of glutaminyl cyclase prevents pGlu-Aβ formation after intracortical/hippocampal microinjection in vivo/in situ. *J. Neurochem. 106*, 1225−1236.

(22) Buchholz, M., Heiser, U., Schilling, S., Niestroj, A. J., Zunkel, K., and Demuth, H. U. (2006) The first potent inhibitors for human glutaminyl cyclase: Synthesis and structure-activity relationship. *J. Med. Chem. 49*, 664−677.

(23) Schilling, S., Lindner, C., Koch, B., Wermann, M., Rahfeld, J. U., Bohlen, A. V., Rudolph, T., Reuter, G., and Demuth, H. U. (2007) Isolation and Characterization of Glutaminyl Cyclases from *Drosophila*: Evidence for Enzyme Forms with Different Subcellular Localization. *Biochemistry 46*, 10921−10930.

(24) Ellis, K. J., and Morrison, J. F. (1982) Buffers of constant ionic strength for studying pH-dependent processes. *Methods Enzymol. 87*, 405−426.

(25) Kabsch, W. (2010) XDS. *Acta Crystallogr. D66*, 125−132.

(26) Evans, P. (2006) Scaling and assessment of data quality. *Acta Crystallogr. D62*, 72−82.

(27) Collaborative Computational Project, Number 4 (1994) The CCP4 suite: Programs for protein crystallography. *Acta Crystallogr. D50*, 760−763.

(28) McCoy, A. J., Grosse-Kunstleve, R. W., Adams, P. D., Winn, M. D., Storoni, L. C., and Read, R. J. (2007) Phaser crystallographic software. *J. Appl. Crystallogr. 40*, 658−674.

(29) Murshudov, G. N., Skubak, P., Lebedev, A. A., Pannu, N. S., Steiner, R. A., Nicholls, R. A., Winn, M. D., Long, F., and Vagin, A. A. (2011) REFMAC5 for the refinement of macromolecular crystal structures. *Acta Crystallogr. D67*, 355−367.

(30) Emsley, P., and Cowtan, K. (2004) Coot: Model-building tools for molecular graphics. *Acta Crystallogr. D60*, 2126−2132.

(31) Kolenko, P., Dohnalek, J., Duskova, J., Skalova, T., Collard, R., and Hasek, J. (2009) New insights into intra- and intermolecular interactions of immunoglobulins: Crystal structure of mouse IgG2b-Fc at 2.1-Å resolution. *Immunology 126*, 378−385.

(32) Chen, V. B., Arendall, W. B., III, Headd, J. J., Keedy, D. A., Immormino, R. M., Kapral, G. J., Murray, L. W., Richardson, J. S., and Richardson, D. C. (2010) MolProbity: All-atom structure validation for macromolecular crystallography. *Acta Crystallogr. D66*, 12−21.

(33) Vaguine, A. A., Richelle, J., and Wodak, S. J. (1999) SFCHECK: A unified set of procedures for evaluating the quality of macromolecular structure-factor data and their agreement with the atomic model. *Acta Crystallogr. D55*, 191−205.

(34) Berman, H. M., Westbrook, J., Feng, Z., Gilliland, G., Bhat, T. N., Weissig, H., Shindyalov, I. N., and Bourne, P. E. (2000) The Protein Data Bank. *Nucleic Acids Res. 28*, 235−242.

(35) Schilling, S., Hoffmann, T., Rosche, F., Manhart, S., Wasternack, C., and Demuth, H. U. (2002) Heterologous expression and

characterization of human glutaminyl cyclase: Evidence for a disulfide bond with importance for catalytic activity. *Biochemistry 41*, 10849−10857.
(36) Carr, P. D., and Ollis, D. L. (2009) α/β hydrolase fold: An update. *Protein Pept. Lett. 16*, 1137−1148.
(37) Grinna, L. S., and Tschopp, J. F. (1989) Size distribution and general structural features of N-linked oligosaccharides from the methylotrophic yeast, *Pichia pastoris*. *Yeast 5*, 107−115.
(38) Jarvis, D. L., and Finn, E. E. (1995) Biochemical analysis of the N-glycosylation pathway in baculovirus-infected lepidopteran insect cells. *Virology 212*, 500−511.
(39) Huang, K. F., Liaw, S. S., Huang, W. L., Chia, C. Y., Lo, Y. C., Chen, Y. L., and Wang, A. H. (2011) Structures of human Golgi-resident glutaminyl cyclase and its complexes with inhibitors reveal a large loop movement upon inhibitor binding. *J. Biol. Chem. 286*, 12439−12449.
(40) Schilling, S., Hoffmann, T., Manhart, S., Hoffmann, M., and Demuth, H. U. (2004) Glutaminyl cyclases unfold glutamyl cyclase activity under mild acid conditions. *FEBS Lett. 563*, 191−196.
(41) Schilling, S., Lauber, T., Schaupp, M., Manhart, S., Scheel, E., Bohm, G., and Demuth, H. U. (2006) On the seeding and oligomerization of pGlu-amyloid peptides (in vitro). *Biochemistry 45*, 12393−12399.
(42) Schlenzig, D., Manhart, S., Cinar, Y., Kleinschmidt, M., Hause, G., Willbold, D., Funke, S. A., Schilling, S., and Demuth, H. U. (2009) Pyroglutamate formation influences solubility and amyloidogenicity of amyloid peptides. *Biochemistry 48*, 7072−7078.
(43) Hartlage-Rubsamen, M., Staffa, K., Waniek, A., Wermann, M., Hoffmann, T., Cynis, H., Schilling, S., Demuth, H. U., and Rossner, S. (2009) Developmental expression and subcellular localization of glutaminyl cyclase in mouse brain. *Int. J. Dev. Neurosci. 27*, 825−835.